

Shading-aware Multi-view Stereo

ECCV 2016 - Supplemental Material

Fabian Langguth¹, Kalyan Sunkavalli²,
Sunil Hadap², and Michael Goesele¹

¹ TU Darmstadt ² Adobe Research

In this document we present some additional results of our algorithm presented in Langguth et al. [1].

- Table 1 shows the quantitative results of our algorithm on the Middlebury benchmark. Reported are the full datasets and algorithms that are also shown in the paper. For detailed results visit the website of the benchmark¹.
- Figure 1 shows another comparison against Zollhoefer et al. [2] on their *Vase* dataset. Similar to the results presented in our paper, our algorithm is able to recover more details and a better overall shape of the object. A .ply file of our reconstruction fused with FSSR [3] can be found in the zip file of this supplemental material and the .ply file of Zollhoefer et al. is available at their project page².
- Figure 2 shows a more global view of the normal maps recovered on the *fountain-p11* dataset by Strecha et al. [4]. These are the same normal maps as shown in Figure 5 in the paper.
- Figure 3 shows a detailed view of our final reconstruction on the *fountain-p11* dataset and a reconstruction using Goesele et al. [5] as implemented in the MVE system [6]. This is also the same view point as in Figure 6 in the paper.
- Figure 4 shows a depth map and our final model of the *herz-jesu-p8* dataset by Strecha et al. [4] compared to the reconstruction by Goesele et al. [5].
- Figure 5 shows more results on the *Owl* dataset where we can observe varying lighting in the input images.

¹<http://vision.middlebury.edu/mview/eval/>

²<http://graphics.stanford.edu/projects/vsfs/>

Algorithm	Temple Full (Acc. - Comp.)	Dino Full (Acc. - Comp.)
Furukawa et al. [7]	0.49mm - 99.6%	0.33mm - 99.8%
Galliani et al. [8]	0.39mm - 99.2%	0.31mm - 99.9%
Semerjian [9]	0.62mm - 97.8%	0.39mm - 99.9%
Fuhrmann et al. [3]	0.39mm - 99.4%	not available
Ours	0.47mm - 98.7%	0.49mm - 96.9%

Table 1: Comparison of quantitative Middlebury evaluations for the figures presented in the main paper.



Figure 1: Comparison against Zollhoefer et al. [2]. *Left*: Input image. *Middle*: Reconstruction by Zollhoefer et al. (available on project page). *Right*: Our reconstruction.



Figure 2: Comparison against basic surface regularization as used by Semerjian [9]. (a) Input image. (b) Normals of our reconstructed depth map for the input image. (c, d, e) Normal of depth maps reconstructed with our implementation of the basic surface regularization by Semerjian [9] for various weights on surface regularization (strong, medium, weak).



Figure 3: Comparison against Goesele et al. [5]. *Left*: Reconstruction using Goesele et al. [5] and FSSR [3] *Middle*: Our reconstruction after fusing depth maps with FSSR. *Right*: Ground truth geometry.

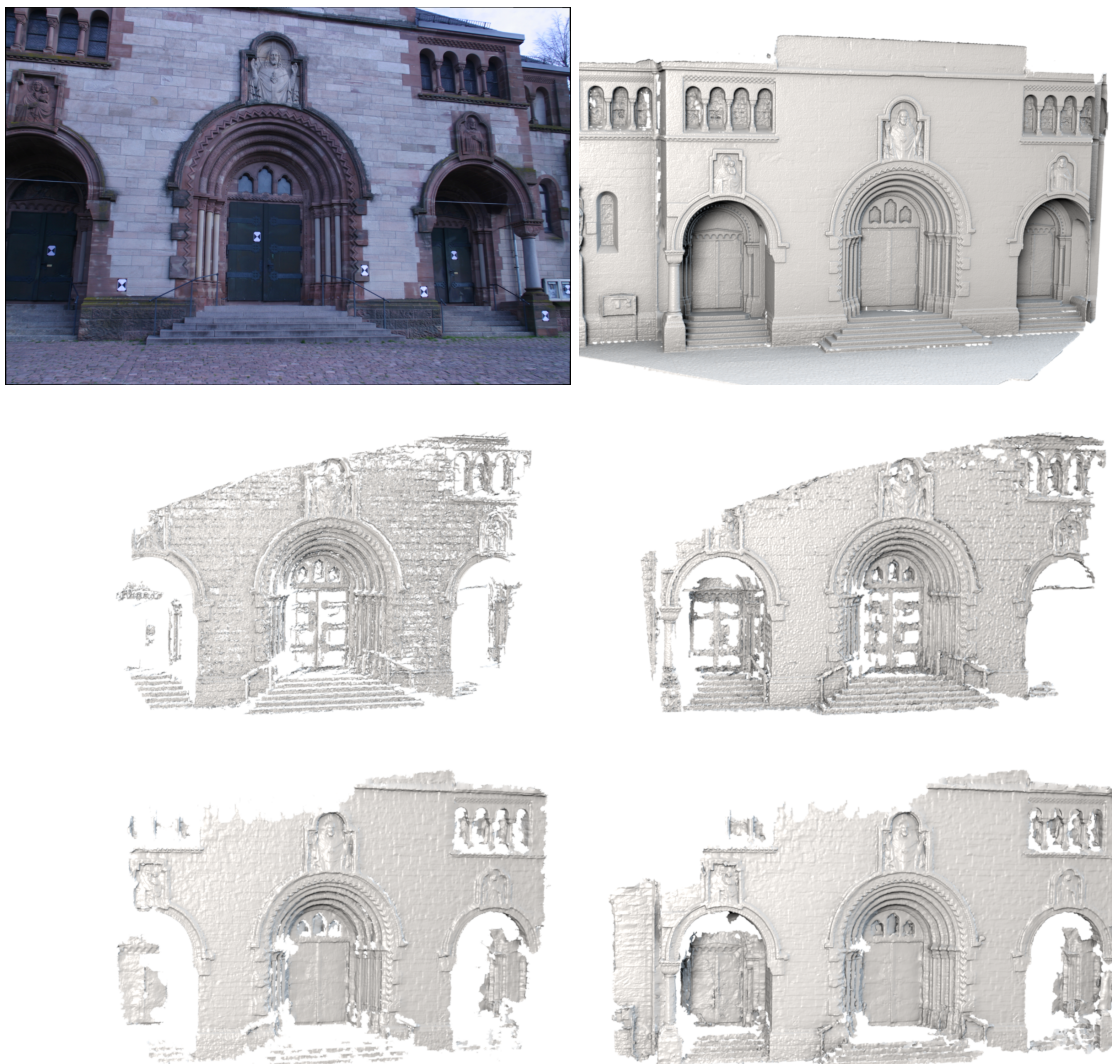


Figure 4: Another comparison against Goesele et al. [5] on the *herz-jesu-p8* from Strecha et al. [4] dataset with 8 images. *Top*: Input image and ground truth geometry. *Middle*: Reconstructed depth map using Goesele et al. [5] and model fused from all 8 images using FSSR [3]. *Bottom*: Our reconstructed depth map and reconstruction after fusing depth maps with FSSR. Our algorithm shows a more complete reconstruction with detailed geometry and less noise.

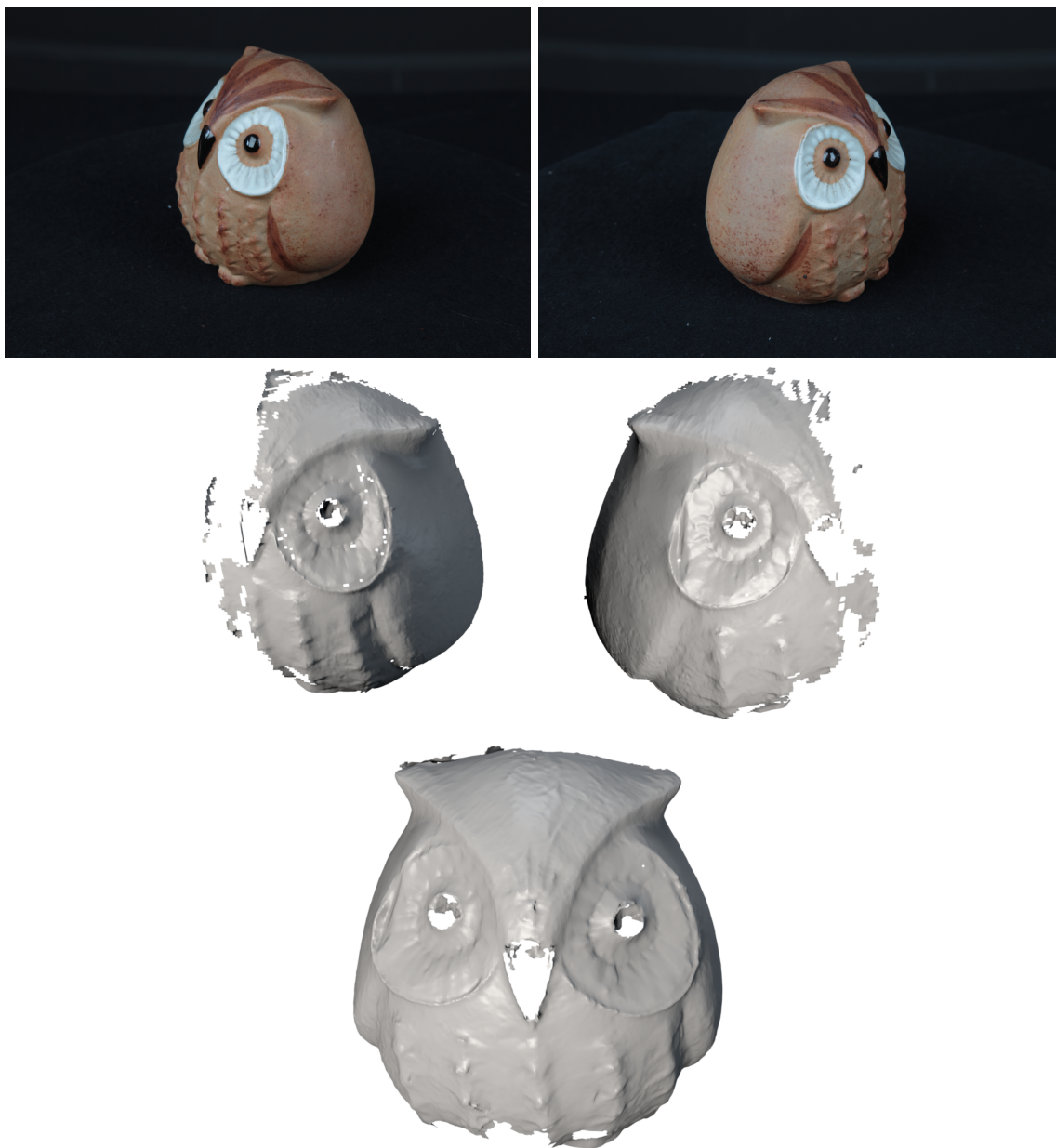


Figure 5: Results on the *Owl* dataset. *Top*: Two additional input images. As the object was captured on a turntable with fixed lights and fixed camera, leading to a different illumination on the object for every image. The specular reflections reveal the light direction to be always behind the camera. *Middle*: Depth maps recovered by our algorithm for the images shown above. *Bottom*: Fused reconstruction using only the two depth maps shown above. Note that the depth maps have been reconstructed for two vastly different viewpoints to the sides of the object. We can observe errors for regions around specular highlights but we still recover a consistent model when viewed from the front.

References

- [1] Langguth, F., Sunkavalli, K., Hadap, S., Goesele, M.: Shading-aware multi-view stereo. In: European Conference on Computer Vision (ECCV). (2016)
- [2] Zollhöfer, M., Dai, A., Innmann, M., Wu, C., Stamminger, M., Theobalt, C., Nießner, M.: Shading-based refinement on volumetric signed distance functions. *ACM Transactions on Graphics (TOG)* (2015)
- [3] Fuhrmann, S., Goesele, M.: Floating Scale Surface Reconstruction. In: Proceedings of ACM SIGGRAPH. (2014)
- [4] Strecha, C., von Hansen, W., Gool, L.V., Fua, P., Thoennessen, U.: On benchmarking camera calibration and multi-view stereo for high resolution imagery. In: Computer Vision and Pattern Recognition, 2008. CVPR 2008. IEEE Conference on. (2008) 1–8
- [5] Goesele, M., Snavely, N., Curless, B., Hoppe, H., Seitz, S.: Multi-View Stereo for Community Photo Collections. In: International Conference on Computer Vision (ICCV). (2007)
- [6] Fuhrmann, S., Langguth, F., Goesele, M.: Mve – a multi-view reconstruction environment. In: Proceedings of the Eurographics Workshop on Graphics and Cultural Heritage (GCH 2014). (2014)
- [7] Furukawa, Y., Ponce, J.: Accurate, Dense, and Robust Multi-View Stereopsis. *Transactions on Pattern Analysis and Machine Intelligence (PAMI)* **32**(8) (2010) 1362–1376
- [8] Galliani, S., Lasinger, K., Schindler, K.: Massively parallel multiview stereopsis by surface normal diffusion. In: 2015 IEEE International Conference on Computer Vision (ICCV). (2015) 873–881
- [9] Semerjian, B.: A new variational framework for multiview surface reconstruction. In: European Conference on Computer Vision (ECCV). (2014) 719–734